Electronic Supplementary Material (ESI) for Soft Matter.
This journal is © The Royal Society of Chemistry 2022

Supporting Information for "Morphologies and dynamics of free surfaces of crystals composed of active particles"

Guoqing Xu,[a,b] Tao Huang,[c] Yilong Han,*[d] and Yong Chen *[a,b]

[a]*Center of Soft Matter Physics and Its Applications, Beihang University, Beijing, 100191, China.*

[b]*School of Physics, Beihang University, Beijing, 100191, China.*

[c]*Institute of Physical and Engineering Science, Faculty of Science,*

Kunming University of Science and Technology, Kunming 650093, Yunnan, China.

[d]*Department of Physics, The Hong Kong University of Science and Technology, Clear Water Bay, Hong Kong, China.*

Movies:

Movie 1: The gas of active particles at $t = 0$ evolves to the steady state of gas-crystal coexistence at $t = 1000$ at $\rho = 0.3$ and $\mathrm{Pe} = 20$.

Movie 2: The gas of active particles at $t = 0$ evolves to the steady state of gas-crystal coexistence at $t = 1000$ at $\rho = 0.3$ and $\mathrm{Pe} = 100$.

Movie 3: The gas of active particles at $t = 0$ evolves to the steady state of gas-crystal coexistence at $t = 1000$ at $\rho = 0.3$ and $\mathrm{Pe} = 200$.

Movie 4: The gas of active particles at $t = 0$ evolves to the steady state of gas-crystal coexistence at $t = 1000$ at $\rho = 0.3$ and $\mathrm{Pe} = 300$.

Movie 5: The gas of active particles at $t = 0$ evolves to the steady state of gas-crystal coexistence at $t = 1000$ at $\rho = 0.3$ and $\mathrm{Pe} = 400$.

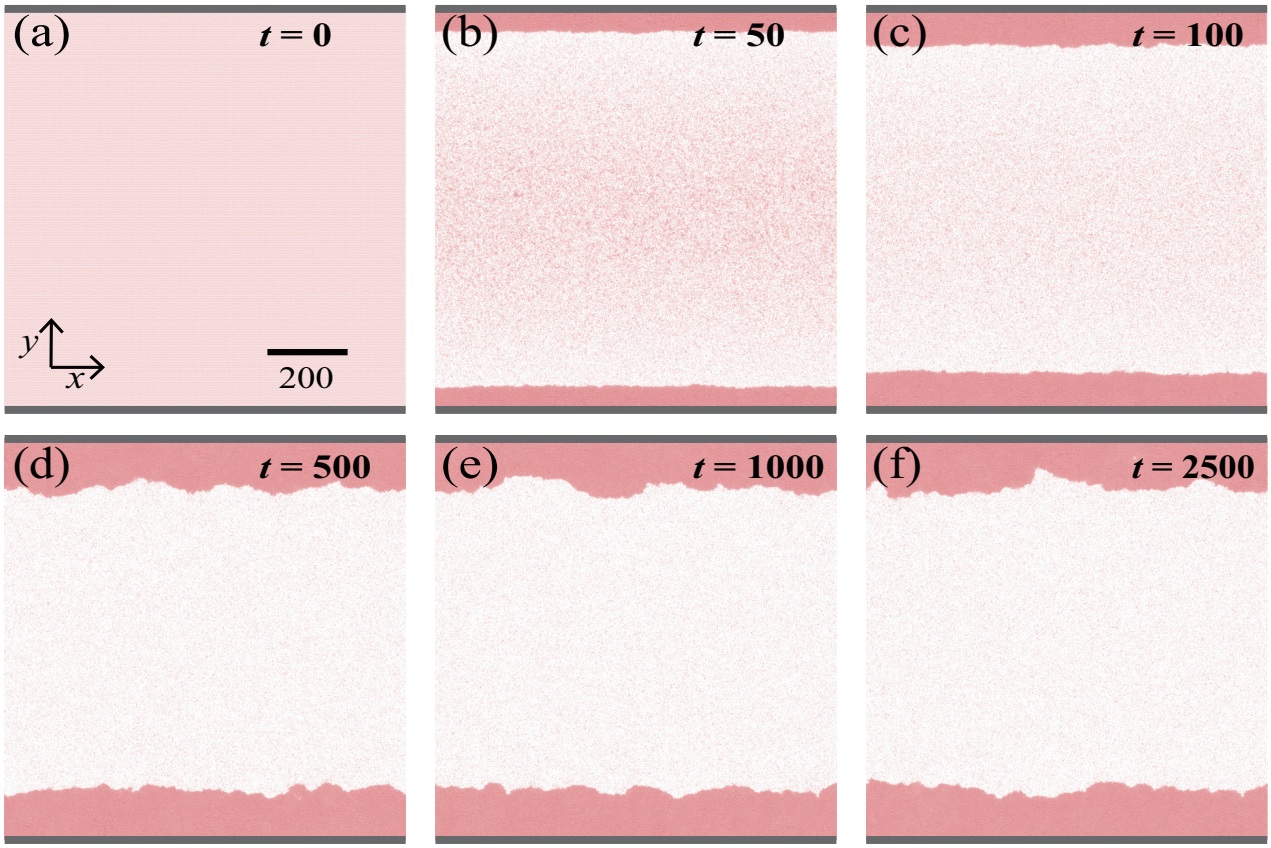

Fig.S1: The formation process of the active crystals at Pe = 400 and $\rho = 0.3$. Its subarea is shown in Fig. 1 in the main text. Particles are 60% of their true diameter in order to be clearly displayed in the dense phase. The top and bottom gray lines represent the two walls.

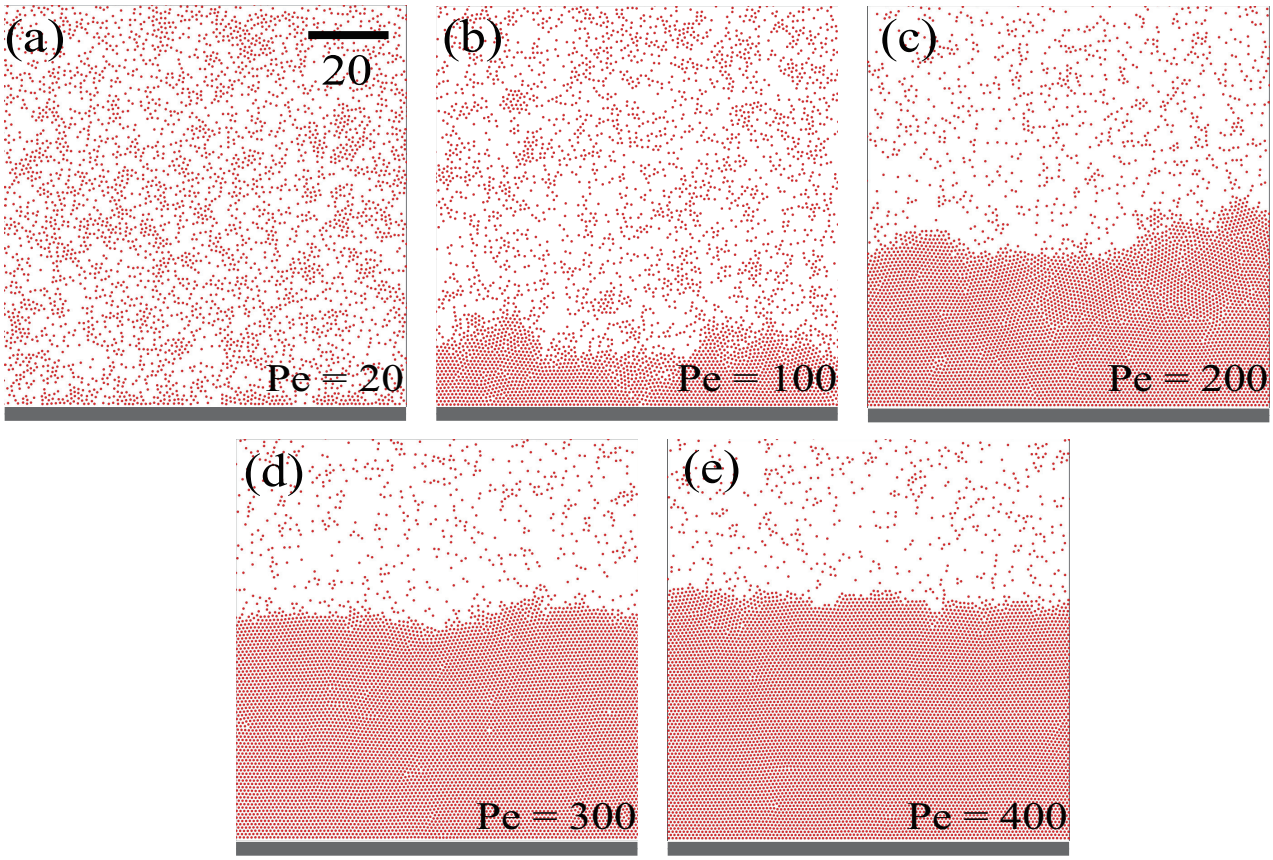

Fig.S2: Five growing active crystals at $\rho = 0.3$, $t = 50$ and different Pe in $l_x \times l_y = 100 \times 100$ subareas. (a) Pe = 20, (b) Pe = 100, (c) Pe = 200, (d) Pe = 300, (e) Pe = 400. Particles are 60% of their true diameter in order to be clearly displayed in the dense phase. The bottom gray line represents the substrate.

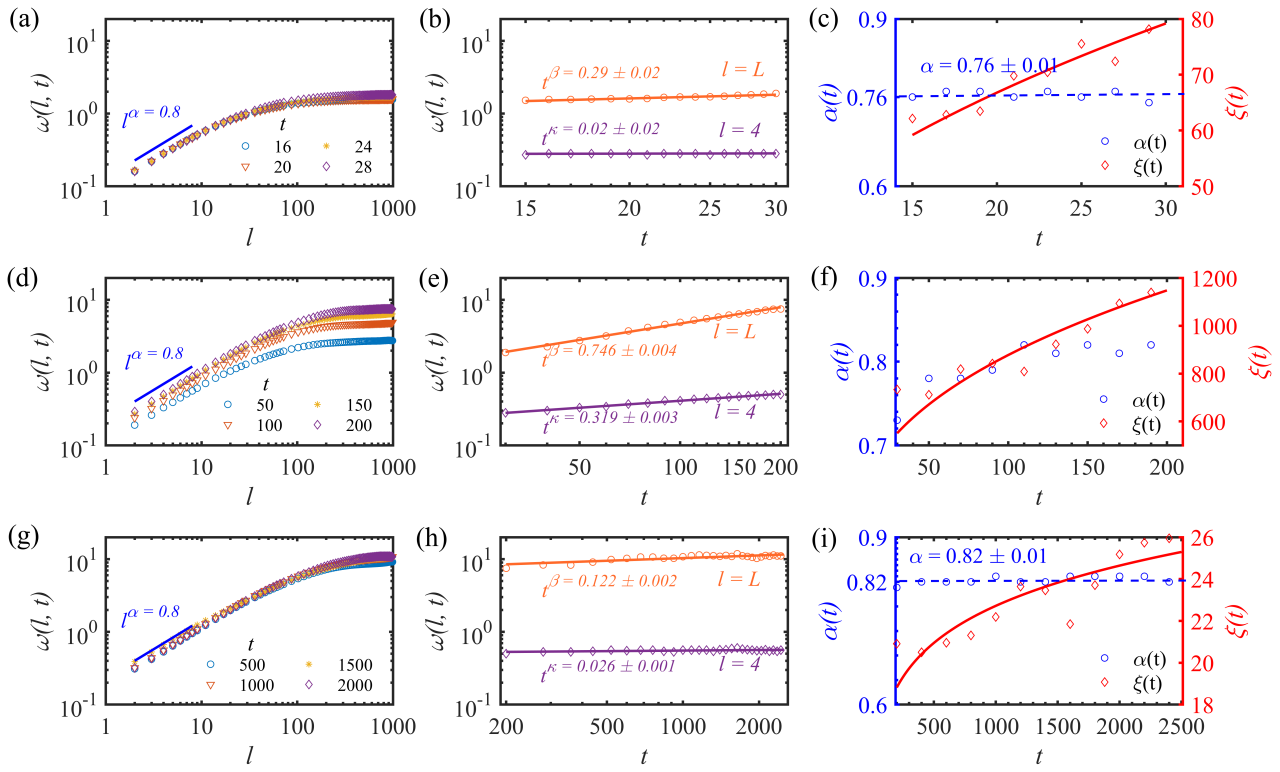

Fig.S3: Three stages of the roughness $\omega(l,t)$ at $(\mathrm{Pe},\rho) = (300, 0.3)$. (a-c), (d-f), and (g-i) correspond to the early, middle and final stages of the blue curves in Fig. 6, respectively. (a, d, g) $\omega(l,t) \sim l^{\alpha}$ at $l \ll \xi(t)$ with $\alpha \approx 0.8$, respectively. (b, e, h) $\omega(l = L,t) \propto t^{\beta}$ for the entire surface with the fitted $\beta = 0.29 \pm 0.02, 0.746 \pm 0.004$ and 0.122 ± 0.002 respectively; and $\omega(l = 4,t) \propto t^{\kappa}$ for short sections of $l = 4$ with the fitted $\kappa = 0.02 \pm 0.02, 0.319 \pm 0.003$ and 0.026 ± 0.001, respectively. (c, f, i) $\alpha(t)$ and $\xi(t)$ obtained by fitting $\omega(l,t)/t^{\beta} = (l/\xi(t))^{\alpha(t)}$ at $l \ll \xi(t)$ in (a), (d), and (g). In the (c) early and (i) final stages, $\alpha(t)$ is nearly a constant 0.76 ± 0.01 and 0.82 ± 0.01, respectively, and $\xi(t) \sim t^{1/z}$ with the fitted $z = 2.38 \pm 0.22$ and 8.53 ± 0.09, respectively. The fitted z values are close to $z = 2.81 \pm 0.30$ and 8.54 ± 0.22 obtained from the scale relation $z = \alpha/(\beta - \kappa)$ for the early and final stages, respectively. However, in the (f) middle stage, $\xi(t) \sim t^{1/z}$ with the fitted $z = 2.58 \pm 0.07$ but $\alpha(t)$ is not a constant. Thus the scale relation $z = \alpha/(\beta - \kappa)$ only holds in the early and final stages. The figure only shows some of the data point but the fittings are based on all the data points, which also appplies to Fig.S5 and Fig.S6.

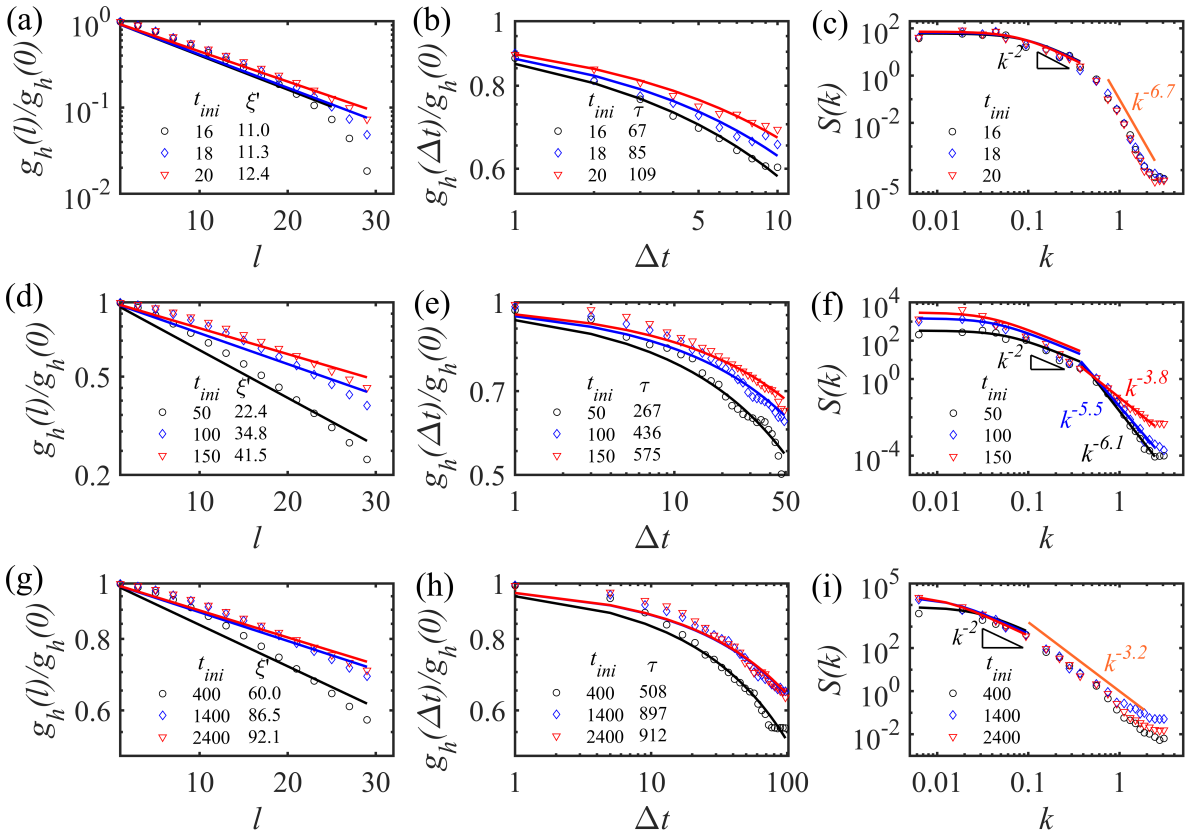

Fig.S4: The normalized spatial and time correlation functions $g_h(l)/g_h(0)$, $g_h(\Delta t)/g_h(0)$, and the power spectrum $S(k)$ of the height function at $(\mathrm{Pe},\rho) = (300, 0.3)$. (a-c), (d-f), and (g-i) are in the early, middle, and final roughening stages, respectively. (a, d, g) $g_h(l)/g_h(0)$ (symbols) fitted with $\exp(-l/\xi')$ (solid curves). (b, e, h) $g_h(\Delta t)/g_h(0)$ (symbols) fitted with $\mathrm{erfc}(\sqrt{\Delta t/\tau})$ (solid curves). (c, f, i) $S(k)$ (symbols) is fitted with $1/(k^2+\xi'^{-2})$ (curves) at small k and deviates from k^{-2} at large k.

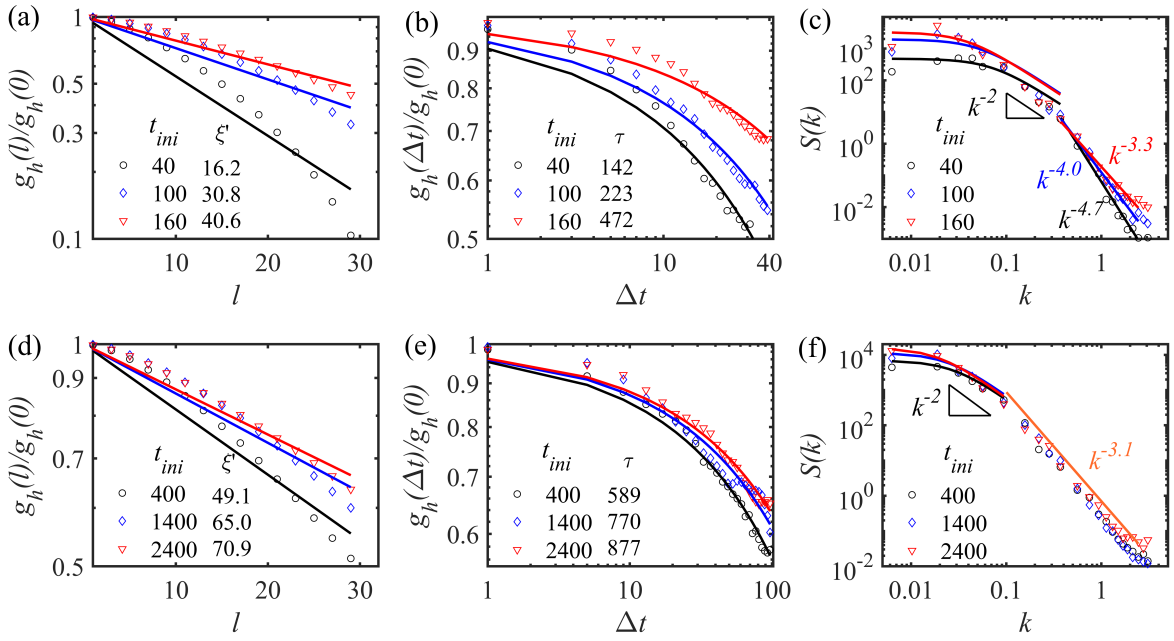

Fig.S5: The normalized spatial and time correlation functions $g_h(l)/g_h(0)$, $g_h(\Delta t)/g_h(0)$, and the power spectrum $S(k)$ of the height function at $(\mathrm{Pe},\rho)=(200,0.3)$. (a-c) and (d-f) are in the middle and final roughening stages, respectively. (a, d) $g_h(l)/g_h(0)$ (symbols) fitted with $\exp(-l/\xi')$ (solid curves). (b, e) $g_h(\Delta t)/g_h(0)$ (symbols) fitted with $\mathrm{erfc}(\sqrt{\Delta t/\tau})$ (solid curves). (c, f) $S(k)$ (symbols) is fitted with $1/(k^2+\xi'^{-2})$ (curves) at small k and deviates from k^{-2} at large k.

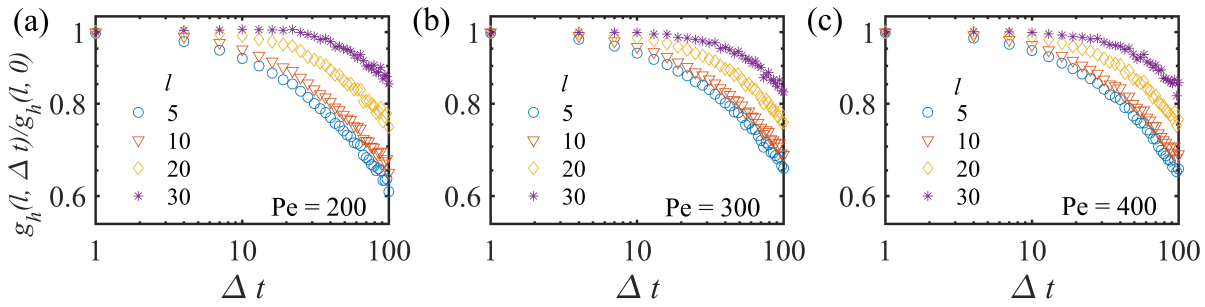

Fig.S6: The normalized time-dependent height-height correlation function $g_h(l,\Delta t)/g_h(l,0)$ at $\rho=0.3$ and different Pe.